Liquid Crystals
Publication details, including instructions for authors and subscription information:
http://www.informaworld.com/smpp/title~content=t713926090

Formation of mesophases by fluorinated enaminoketone Ni(II), Cu(II) and VO(II) complexes

Jadwiga Szydłowska[a]; Adam Krówczyński[a]; Urszula Pietrasik[a]; Agnieszka Rogowska[a]
[a] Department of Chemistry, Warsaw University, Laboratory of Dielectrics and Magnetics, 02-089 Warsaw, Poland

To cite this Article Szydłowska, Jadwiga , Krówczyński, Adam , Pietrasik, Urszula and Rogowska, Agnieszka(2005) 'Formation of mesophases by fluorinated enaminoketone Ni(II), Cu(II) and VO(II) complexes', Liquid Crystals, 32: 5, 651 — 658

To link to this Article: DOI: 10.1080/02678290500125459

URL: http://dx.doi.org/10.1080/02678290500125459

Liquid Crystals, Vol. 32, No. 5, May 2005, 651–658

Formation of mesophases by fluorinated enaminoketone Ni(II), Cu(II) and VO(II) complexes

JADWIGA SZYDŁOWSKA*, ADAM KRÓWCZYŃSKI, URSZULA PIETRASIK and
AGNIESZKA ROGOWSKA

Department of Chemistry, Warsaw University, Laboratory of Dielectrics and Magnetics, Al. Żwirki i Wigury 101, 02-089 Warsaw, Poland

(*Received 29 October 2004; in final form 14 February 2005; accepted 21 February 2005*)

Mesogenic tetradentate *cis*-enaminoketone Ni(II), Cu(II) and VO(II) complexes with rod-like and disc-like molecular shapes were synthesized. In these compounds some of the alkyl chains were perfluorinated. Replacing the alkyl chains by fluorinated chains stabilizes the columnar hexagonal $\mathrm{Col_h}$ phase whereas lamellar phases are destroyed.

1. Introduction

Compounds containing fluorocarbon chains are of increasing interest because of their influence on the self-segregation mechanism which results in the appearance of liquid crystalline phases. Supramolecular organization can be easily induced through the fluorophobic effect [1], arising from the incompatibility of fluorinated and non-fluorinated hydrocarbons [2, 3]. The incompatibility results from differences in the cohesive energy between perfluoroalkyl chains and hydrocarbon chains. Incorporating perfluorinated alkyl chains into classical calamitic and discotic molecules leads to microsegregation and in many cases, increases the stability of smectic and columnar phases, respectively, in comparison with the hydrocarbon analogues [4–6]. There are many non-conventional liquid crystals whose mesomorphic properties are significantly influenced by fluorination. These substances include polycatenar compounds [7], imine-based metallomesogens [8], banana-shaped mesogens [9] and bolaamphiphile mesogens [10]. It was shown also that the introduction of perfluorocarbon chains into polysiloxanes promotes smectic properties and stabilizes the layer structure in a multilayer LB film [11]. In pentaerythritol tetrabenzoate, replacing the alkyl chains by a mixed system of fluocarbon and hydrocarbon chains also favours the columnar $\mathrm{Col_h}$ phase, although in this case the fluorinated and non-fluorinated chains are not separated in the phase [12, 13].

In order to examine the influence of fluorination on the tetradentate *cis*-enaminoketone complexes, three series of liquid-crystalline compounds, **I**, **II** and **III** bearing hydrocarbon and perfluorinated chains were synthesized (scheme 1) [14–16]. In these compounds the structure of the mesogenic core is almost triangular and similar to those reported earlier. It contains two *cis*-enaminoketone rings and three phenyl rings. At the aminophenyl ring two terminal octyloxy chains are attached. In each series the R_1, R_2 or R moieties in the *para*- positions of both aroyl rings were varied, and octyl, octyloxy or fluorocarbon chains used.

In comparison with series **I**, in the complexes of series **II**, two additional heptyl chains are attached at the α-carbon atoms of the *cis*-enaminoketone parts, whereas for series **III** the octyloxy chain is joined to the aminophenyl ring in the 3-position. These substituents broaden the molecular shape. For the series I, only Ni complexes have been synthesized, while for the series **II** and **III** Cu and VO complexes have also been obtained.

2. Experimental

2.1. *Synthesis*

The synthetic procedure used to obtain the complexes of series **I**, having identical or different terminal chains (R_1 and R_2), is shown in scheme 2. The starting materials are known and their synthesis routine. Formyl ketone sodium salts **3** were obtained by the Claisen formylation reaction. 4,5-Dioctyloxy-1,2-phenylenediamine **2** (1 mmol) and the sodium salt of formyl ketone **3** (1 mmol) dissolved in methanol (100 ml) and neutralized with acetic acid (to pH about 6), reacted at room temperature selectively. The aroylvinyl group was joined to only one of the amino groups resulting in a

---

*Corresponding author. Email: jadszyd@chem.uw.edu.pl

Liquid Crystals
ISSN 0267-8292 print/ISSN 1366-5855 online © 2005 Taylor & Francis Group Ltd
http://www.tandf.co.uk/journals
DOI: 10.1080/02678290500125459

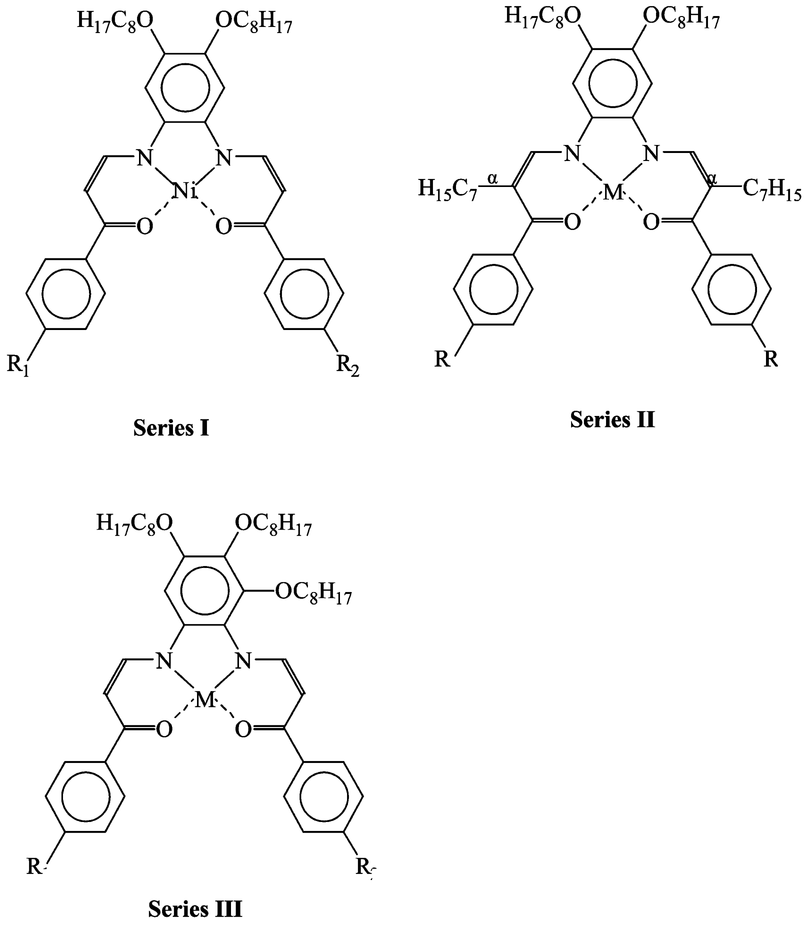

Series I

Series II

Series III

Scheme 1. Structures of the compounds synthesized.

crystalline intermediate **4**, which was purified by recrystallization from octane (yield ~ 80%). The remaining amino group of compound **4** was reacted further with a formyl ketone derivative **5** (1 mmol) at the boiling point of ethanol (50 ml) giving the tetradentate ligand **6** after 10 min. A metal salt — nickel(II) acetate — dissolved in hot ethanol (15 ml) was added to the boiling mixture. After 5 min of reflux the mixture was cooled resulting in the precipitate of compound **1**, which was filtered off. The product **1** was recrystallized from hexane and then chromatographed on silica gel, eluted with hexane/methylene chloride solvents (1/1). For the symmetrical ligands ($R_1 = R_2$), 4,5-dioctyloxy-1,2-phenylenediamine **2** (1 mmol) and the sodium salt of formyl ketone **3** (3.3 mmol) were reacted to give **6** immediately.

To obtain the complexes of series **II** the same synthetic procedure was applied using the appropriate formyl ketone salt. In the case of series **III**, 3,4,5-trioctyloxy-1,2-phenylenediamine was used. Cu(OAc)$_2$ and VO(acac)$_2$ were added instead of Ni(OAc)$_2$ to obtain complexes containing different metal ions.

2.2. *Elemental analyses and NMR spectra*

The C, H, N, elemental analyses for the complexes obtained were satisfactory, and are listed below. The ^{1}H NMR spectra for Ni complexes (in CDCl$_3$) are consistent with the proposed structures with no sign of additives or impurities.

I-1: Calculated for C$_{56}$H$_{82}$O$_5$N$_2$Ni (921.97), C 72.95, H 8.96, N 3.04; found, C 72.96, H 8.93, N 3.07%. ^{1}H NMR (CDCl$_3$): $\delta = 0.86$–1.84 (m, 60 H, (CH$_2$)$_7$H); 2.64 (t, $J = 7.6$ Hz, 2H, CH$_2$); 3.99 (t, $J = 6.6$ Hz, 4H) and 4.03 (t, $J = 6.6$ Hz, 2H)–OCH$_2$; 6.12 (d, $J = 6.6$ Hz, 1H) and 6.17 (d, $J = 6.6$ Hz, 1H)–H^{2I}, H^{2II}; 6.91 and 7.89 (AA'BB', $J = 8.6$ Hz, 4H, H^{2IV}, H^{3IV}, H^{5IV}, H^{6IV}); 6.96 (s, 1H) and 6.98 (s, 1H)–H^3, H^6; 7.24 and 7.85 (AA'BB', $J = 8.3$ Hz, 4H, H^{2III}, H^{3III}, H^{5III}, H^{6III}); 7.42 (d, $J = 6.6$ Hz, 1H) and 7.46 (d, $J = 6.6$ Hz, 1H)–H^{1I}, H^{1II}. ^{13}C NMR (CDCl$_3$): $\delta = 14.13$, 22.68, 22.69, 26.03,

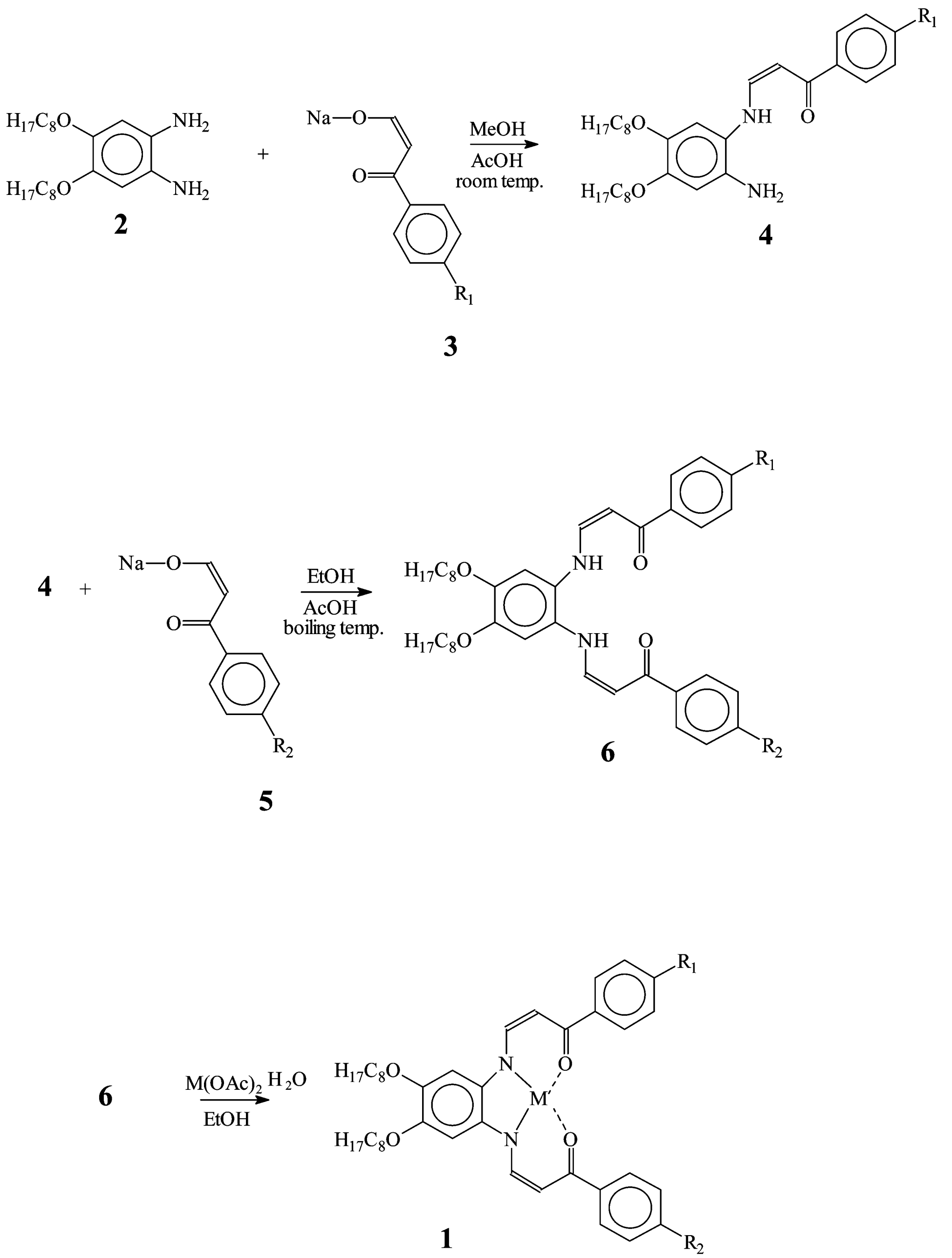

Scheme 2. Synthetic route used to obtain the tetradentate *cis*-enaminoketone complexes.

26.05, 29.22, 29.25, 29.27, 29.30, 29.35, 29.37, 29.21, 29.48, 31.26, 31.82, 31.85, 31.89, 35.91, 68.10, 69.95, 69.99, 94.35, 94.86, 98.96, 99.06, 114.07, 126.94, 128.37, 128.69, 129.35, 134.48, 136.05, 136.30, 145.65, 146.25, 146.38, 146.93, 147.11, 161.18, 173.75, 174.

I-2: Calculated for $C_{56}H_{82}O_6N_2Ni$ (937,97), C 71.70, H 8.81, N 2.98; found, C 71.33, H 8.86, N 3.10%. ^{1}H NMR ($CDCl_3$): $\delta = 0.88–1.84$ (m, 60 H, $(CH_2)_7H$); 3.98 (t, $J = 6.6$ Hz, 4H) and 4.01 (t, $J = 6.6$ Hz, 4H)–OCH_2; 6.13 (d, $J = 6.8$ Hz, 2H, H^{2I}); 6.89 (s, 2H, H^3, H^6); 6.92 and 7.90 (AA'BB', $J = 8.8$ Hz, 8H, H^{2II}, H^{3II}, H^{5II}, H^{6II}); 7.42 (d, $J = 6.8$ Hz, 2H, H^{1I}). ^{13}C NMR ($CDCl_3$): $\delta = 14.12$; 14.13; 22.68; 22.69; 26.05; 26.07; 29.24; 29.26; 29.31; 29.38; 29.42; 31.83; 31.85; 68.11; 69.99; 94.35; 99.04; 114.07; 128.66; 129.42; 136.21; 146.22; 146.97; 161.19; 173.65.

I-3: Calculated for $C_{56}H_{82}O_4N_2Ni$ (905.97), C 74.24, H 9.12, O 7.06, N 3.09; found, C 74.26, H 9.10, N 3.12%. ^{1}H NMR ($CDCl_3$): $\delta = 0.88–1.84$ (m, 60 H, $(CH_2)_7H$); 2.64 (t, $J = 8.1$ Hz, 4H, CH_2); 3.96 (t, $J = 6.6$ Hz, 4H, OCH$_2$); 6.36 (d, $J = 6.7$ Hz, 2H, H^{2I}); 6.98 (s, 2H, H^3, H^6); 7.44 (d, $J = 6.7$ Hz, 2H, H^{1I}); 7.21 and 7.86 (AA'BB', $J = 8.2$ Hz, 8H, H^{2II}, H^{3II}, H^{5II}, H^{6II}). ^{13}C NMR (CDCl$_3$): $\delta = 14.12$, 22.68, 22.69, 26.06, 29.27, 29.31, 29.36, 29.42, 29.49, 31.25, 31.85, 31.89, 35.92, 69.95, 94.86, 99.00, 126.97, 128.36, 134.45, 136.16, 145.67, 146.39, 147.09, 174.11.

I-4: Calculated for $C_{56}H_{48}O_4N_2F_{34}Ni$ (1517.63), C 44.32, H 3.19, N 1.84, F 42.56; found, C 44.98, H 3.68, N 2.10, F 42.53%. ^{1}H NMR (CDCl$_3$): $\delta = 0.88$–1.82 (m, 30 H, (CH$_2$)$_7$H); 3.98 (t, $J = 6.6$ Hz, 4H, OCH$_2$); 6.22 (d, $J = 6.3$ Hz, 2H, H^{2I}); 7.00 (s, 2H, H^3, H^6); 7.52 (d, $J = 6.3$ Hz, 2H, H^{1I}); 7.64 and 8.00 (AA'BB', $J = 8.6$ Hz, 8H, H^{2II}, H^{3II}, H^{5II}, H^{6II}). ^{13}C NMR (CDCl$_3$): $\delta = 14.12$, 22.69, 26.05, 29.29, 29.39, 31.84, 69.92, 76.45, 95.83, 98.84, 126.98, 135.98, 140.14, 147.03, 147.83, 171.95.

I-5: Calculated for $C_{56}H_{65}O_4N_2F_{17}Ni$ (1211.80), C 55.50, H 5.40, N 2.31, F 26.65; found, C 55.54, H 5.43, N 2.38, F 26.69%. ^{1}H NMR (CDCl$_3$): $\delta = 0.86$–1.86 (m, 45 H, (CH$_2$)$_7$H); 2.44 (t, $J = 7.8$ Hz, 2H, CH$_2$); 3.94–4.04 (m, 4H, OCH$_2$); 6.18 (d, $J = 6.3$ Hz, 1H) and 6.21 (d, $J = 6.3$ Hz, 1H)–H^{2I}, H^{2II}; 6.96 (s, 1H) and 7.0 (s, 1H)–H^3, H^6; 7.23 and 8.03 (AA'BB', $J = 8.3$ Hz, 4H, H^{2III}, H^{3III}, H^{5III}, H^{6III}); 7.43 and 7.54 (AA'BB', $J = 6.8$ Hz, 4H, H^{2IV}, H^{3IV}, H^{5IV}, H^{6IV}); 7.64 (d, $J = 6.3$ Hz, 1H) and 7.84 (d, $J = 6.3$ Hz, 1H)–H^{1I}, H^{1II}. ^{13}C NMR (CDCl$_3$): $\delta = 14.12$, 22.69, 26.05, 29.30, 29.40, 29.47, 31.24, 31.84, 35.91, 69.85, 70.00, 95.03, 95.84, 98.73, 99.07, 126.98, 127.56, 128.46, 134.21, 135.56, 136.57, 140.34, 146.01, 146.58, 146.84, 147.13, 147.77, 171.54, 174.51.

I-6: Calculated for $C_{56}H_{65}O_5N_2F_{17}Ni$ (1227.8), C 54.78, H 5.34, N 2.28, F 26.30; found, C 54.75, H 5.38, N 2.24, F 26.35%. ^{1}H NMR (CDCl$_3$): $\delta = 0.88$–1.88 (m, 45 H, (CH$_2$)$_7$H); 3.94–3.98 (m, 4H) I 4.02 (t, $J = 6.3$ Hz, 2H)–OCH$_2$; 6.12 (d, $J = 6.3$ Hz, 1H) and 6.18 (d, $J = 6.3$ Hz, 1H)–H^{2I}, H^{2II}; 6.92 (s, 1H) and 6.94 (s, 1H)–H^3, H^6; 7.38 (d, $J = 6.3$ Hz, 1H) and 7.52 (d, $J = 6.3$ Hz, 1H)–H^{1I}, H^{1II}; 6.97 and 8.00 (AA'BB', $J = 8.3$ Hz, 4H, H^{2III}, H^{3III}, H^{5III}, H^{6III}); 7.60 and 7.88 (AA'BB', $J = 6.8$ Hz, 4H, H^{2IV}, H^{3IV}, H^{5IV}, H^{6IV}). ^{13}C NMR (CDCl$_3$): $\delta = 14.12$, 22.70, 26.03, 26.07, 29.25, 29.31, 29.37, 29.42, 31.85, 68.14, 69.80, 70.00, 94.49, 95.69, 98.62, 99.09, 114.13, 126.95, 128.71, 129.10, 135.45, 136.70, 140.40, 146.32, 146.71, 146.94, 147.76, 161.36, 171.31, 174.00.

II-1: Calculated for $C_{70}H_{110}O_4N_2Ni$ (1102.35), C 76.27, H 10.05, N 2.54; found, C 76.31, H 10.09, N 2.59%. ^{1}H NMR (CDCl$_3$): $\delta = 0.82$–1.88 (m, 86 H, (CH$_2$)$_7$H); 2.36 (t, $J = 8.0$ Hz, 4H) and 2.58 (t, $J = 7.7$ Hz, 4H)–CH$_2$; 4.02 (t, $J = 6.6$ Hz, 4H, OCH$_2$); 7.01 (s, 2H, H^3, H^6); 7.10 and 7.32 (AA'BB', $J = 8.2$ Hz, 8H, H^{2II}, H^{3II}, H^{5II}, H^{6II}); 7.46 (s, 2H, H^{1I}). ^{13}C NMR (CDCl$_3$): $\delta = 14.09$, 14.12, 22.64, 22.67, 22.69, 26.11, 28.97, 28.98, 29.26, 29.28, 29.31, 29.43, 29.46, 31.31, 31.80, 31.84, 31.89, 33.07, 35.83, 70.22, 99.46, 108.99, 127.66, 127.88, 136.36, 136.80, 143.44, 147.05, 149.31, 177.68.

II-2: Calculated for $C_{70}H_{76}O_4N_2F_{34}Ni$ (1714.01), C 49.05, H 4.47, N 1.63, F 37.68; found, C 49.07, H 4.51, N 1.68, F 37.62%. ^{1}H NMR (CDCl$_3$): $\delta = 0.82$–1.88 (m, 56 H, (CH$_2$)$_7$H); 2.31 (t, $J = 7.7$ Hz, 4H, CH$_2$); 4.04 (t, $J = 6.7$ Hz, 4H, OCH$_2$); 7.02 (s, 2H, H^3, H^6); 7.48 (s, 2H, H^{1I}); 7.50–7.56 (m, 8H, H^{2II}, H^{3II}, H^{5II}, H^{6II}). ^{13}C NMR (CDCl$_3$): δ = 14.00, 14.12, 22.57, 22.70, 26.12, 28.90, 28.92, 29.32, 29.42, 29.44, 30.99, 31.75, 31.85, 33.04, 70.15, 99.28, 109.28, 126.42, 128.17, 136.12, 142.84, 147.71, 149.88, 175.08.

II-3: Calculated for $C_{70}H_{76}O_4N_2F_{34}Cu$ (1718.87), C 48.91, H 4.45, N 1.63, F 37.57; found, C 48.97, H 4.42, N 1.69, F 37.51%.

II-4: Calculated for $C_{70}H_{76}O_5N_2F_{34}V$ (1722.26), C 48.81, H 4.45, N 1.62, F 37.50; found, C 48.86, H 4.41, N 1.67, F 37.58%.

III-1: Calculated for $C_{64}H_{98}O_5N_2Ni$ (1034.19), C 74.32, H 9.55, N 2.71; found, C 74.78, H 9.10, N 2.31%. ^{1}H NMR (CDCl$_3$): $\delta = 0.86$–1.86 (m, 75 H, (CH$_2$)$_7$H); 2.62 (t, $J = 7.5$ Hz, 4H, CH$_2$); 3.92–3.98 (m, 4H) and 4.02 (t, $J = 6.6$ Hz, 2H)–OCH$_2$; 6.12 (d, $J = 6.8$ Hz, 1H) and 6.18 (d, $J = 6.8$ Hz, 1H)–H^{2I}, H^{2II}; 6.78 (s, 1H, H^6); 7.16–7.24 (m, 4H) and 7.86–7.94 (m, 4H)–H^{2III}, H^{3III}, H^{5III}, H^{6III}, H^{2IV}, H^{3IV}, H^{5IV}, H^{6IV}; 7.50 (d, $J = 6.8$ Hz, 1H) and 8.68 (d, $J = 6.8$ Hz, 1H)–H^{1I}, H^{1II}. ^{13}C NMR (CDCl$_3$): $\delta = 14.12$, 22.68, 22.70, 26.12, 26.19, 29.26, 29.28, 29.35, 29.37, 29.38, 29.44, 29.47, 29.55, 30.21, 30.36, 31.23, 31.25, 31.84, 31.86, 31.88, 35.91, 69.06, 73.77, 74.15, 92.93, 95.08, 95.19, 126.98, 127.02, 128.32, 128.40, 129.62, 134.36, 139.37, 139.59, 145.23, 145.51, 145.87, 146.78, 149.48, 153.39, 172.67, 174.91.

III-2: Calculated for $C_{64}H_{98}O_7N_2Ni$ (1066.70), C 72.01, H 9.26, N 2.63; found, C 71.82, H 8.84, N 2.19%. ^{1}H NMR (CDCl$_3$): $\delta = 0.86$–1.86 (m, 75 H, (CH$_2$)$_7$H); 3.92–3.98 (m, 6H) and 4.02 (t, $J = 6.6$ Hz, 4H)–OCH$_2$; 6.06 (d, $J = 6.6$ Hz, 1H) and 6.12 (d, $J = 6.6$ Hz, 1H)–H^{2I}, H^{2II}; 6.76 (s, 1H, H^6); 6.85–6.93 (m, 4H) and 7.86–7.94, (m, 4H)–H^{2III}, H^{3III}, H^{5III}, H^{6III}, H^{2IV}, H^{3IV}, H^{5IV}, H^{6IV}; 7.46 (d, $J = 6.6$ Hz, 1H) and 8.66 (d, $J = 6.6$ Hz, 1H)–H^{1I}, H^{1II}. ^{13}C NMR (CDCl$_3$): $\delta = 14.12$, 22.67, 22.70, 26.04, 26.12, 26.19, 29.22, 29.25, 29.30, 29.37, 29.44, 29.56, 30.21, 30.37, 31.82, 31.84, 31.86, 31.90, 68.09, 69.08, 73.73, 74.15, 92.92, 94.67, 114.04, 114.11, 128.66, 128.75, 129.33, 129.35, 129.63, 139.41, 139.48, 145.17, 146.57, 149.36, 153.19, 161.04, 161.27, 172.20, 174.41.

III-3: Calculated for $C_{64}H_{64}O_5N_2F_{34}Ni$ (1645.85), C 46.70, H 3.92, N 1.70, F 39.24; found, C 46.23, H 3.30, N 1.89, F 39.68%. ^{1}H NMR ($CDCl_3$): $\delta = 0.86$–1.88 (m, 45 H, $(CH_2)_7H$); 3.94–3.99 (m, 4H) and 4.04 (t, $J = 6.5$ Hz, 2H)–OCH_2; 6.16 (d, $J = 6.3$ Hz, 1H) and 6.22 (d, $J = 6.3$ Hz, 1H)–H^{2I}, H^{2II}; 6.80 (s, 1H, H^6); 7.56 (d, $J = 6.3$ Hz, 1H) and 8.78 (d, $J = 6.3$ Hz, 1H)–H^{1I}, H^{1II}; 7.62–7.68 (m, 4H) and 8.00–8.08 (m, 4H)–H^{2III}, H^{3III}, H^{5III}, H^{6III}, H^{2IV}, H^{3IV}, H^{5IV}, H^{6IV}. ^{13}C NMR ($CDCl_3$): $\delta = 14.09$, 14.12, 22.70, 26.13, 26.19, 29.30, 29.36, 29.38, 29.43, 29.55, 30.24, 30.37, 31.85, 31.86, 31.90, 69.09, 73.97, 74.20, 76.52, 92.96, 96.01, 96.23, 108.54, 110.85, 116.00, 118.27, 126.99, 127.03, 129.53, 130.10, 130.38, 139.18, 140.11, 140.25, 144.73, 145.51, 147.57, 150.18, 154.15, 170.42, 172.71, 190.39.

III-4: Calculated for $C_{64}H_{64}O_5N_2F_{34}Cu$ (1650.70), C 46.56, H 3.91, N 1.69, F 39.13; found, C 46.08, H 3.32, N 1.35, F 39.19%.

III-5: Calculated for $C_{64}H_{64}O_6N_2F_{34}V$ (1670.10), C 46.02, H 3.86, N 1.68, F 38.67; found, C 45.67, H 3.23, N 2.03, F 38.04%.

2.3. *Measurements*

The mesophases were identified by the microscopic examination of the liquid crystalline textures. A Zeiss Jenapol-U polarizing microscope equipped with a Mettler FP82HT hot stage was used. Phase transition temperatures were mainly determined by calorimetric measurements performed using a Perkin-Elmer DSC-7 at a scanning rate of 5 K min^{-1}. When the signal from the DSC was very broad, the temperatures were taken from microscopic observations. The NMR spectra were recorded using a Varian Unity Plus spectrometer operating at 500 MHz. For some compounds, in order to study the mesophase structure, X-ray studies were performed using a DRON spectrometer. Molecular dimensions were estimated by molecular modelling using Hyperchem.

3. Results and discussion

The mesomorphic properties, phase sequences, transition temperatures and enthalpy changes of the compounds synthesized are summarized in tables 1, 2 and 3. Enantiotropic columnar as well as smectic phases were observed.

The molecular shape of the complexes of series **I**, containing octyl and/or octyloxy chains as the R_1 and R_2 substituents (**I-1**, **I-2**), was shown to be rod-like [16], which enables the formation of smectic phases. The mesophase properties are enhanced for the complex with mixed chains **I-1** compared with the symmetrical octyloxy compound (**I-2**), which exhibits only a monotropic smectic A phase [14]. It appears that the appearance of the orthogonal SmA phase is connected with having two terminal alkoxy chains, which make the molecules stiffer than with alkyl groups. Introducing greater flexibility in compound **I-1** by substituting one alkoxy chain provides the greatest ability for the molecules to form zig-zag shapes which promotes the SmC phase. Also, the non-symmetry in the molecules

Table 1. Melting points, phase sequences, transition temperatures (in °C), and associated enthalpy changes (in parenthesis, J g^{-1}) for series **I**.

Compound	R_1	R_2	Melting point	Phase sequence and transition temperatures
I-1	C_8H_{17}	OC_8H_{17}	86.9 (12.8)	SmC–111.8 (8.4)–I
I-2[c]	OC_8H_{17}	OC_8H_{17}	137.2 (37.6)	SmA–122.2[a]–I
I-3	C_8H_{17}	C_8H_{17}	135.3[b]	—
I-4	C_8F_{17}	C_8F_{17}	180[b]	—
I-5	C_8F_{17}	C_8H_{17}	135.3 (5.2)	—
I-6	C_8F_{17}	OC_8H_{17}	147.3 (0.6)	—

[a] From microscopy.

[b] From microscopy – broad signal from DSC scanning calorimeter.

[c] From [14].

Table 2. Melting points, phase sequences, transition temperatures (in °C), and associated enthalpy changes (in parenthesis, J g^{-1}) for series **II**.

Compound	M	R	Melting point	Phase sequence and phase transition temperatures
II-1	Ni	C_8H_{17}	100.8 (17.5)	—
II-2	Ni	C_8F_{17}	109.8 (15.2)	Col_h–158.0 (2.9)–I
II-3	Cu	C_8F_{17}	59.6 (6.5)	Col_h–188.5 (5.0×10^{-2})–I
II-4	VO	C_8F_{17}	105.4 (9.5)	—

Table 3. Melting points, phase sequences, transition temperatures (in °C), and associated enthalpy changes (in parenthesis, J g^{-1}) for series **III**.

Compound	*M*	*R*	Melting point	Phase sequence and phase transition temperatures
III-1	Ni	C_8H_{17}	51.3 (2.3)	—
III-2	Ni	OC_8H_{17}	70.6 (24.3)	—
III-3	Ni	C_8F_{17}	115.6 (14.1)	Col_h–253.7 (2.9)–I
III-4	Cu	C_8F_{17}	below room temp.	Col_h–266.0 (4.5)–I
III-5	VO	C_8F_{17}	68.5 (16.9)	Col_h–173.2 (1.1)–I

results in the lowering of the melting points and the appearance of the enantiotropic smectic C phase. However, further modification of the terminal chains, i.e. R_1 and R_2 octyl (**I-3**), perfluorinated (**I-4**) or mixed (**I-5**, **I-6**) chains, does not result in the formation of liquid crystalline phases. These complexes have relatively high melting temperatures, especially **I-4** which contains two perfluorinated chains.

The molecules of series **II**, with a molecular contour broadened by the heptyl chains, may be expected to form columnar phases. However, the Ni complex **II-1** containing two octyl chains is not mesogenic, despite the disc-like molecular shape and the relatively low melting point. The related complexes having two perfluorinated chains (Ni, **II-2**; Cu, **II-3**) exhibit a hexagonal columnar Col_h phase over a broad temperature range, due to high clearing temperatures.

In series **III** the deformation of the rod-like molecular shape by attaching the octyloxy group at the aminophenyl fragment, suppresses liquid crystalline behaviours for the complexes having octyl (**III-1**) and octyloxy (**III-2**) terminal *R* chains. Replacing these chains by fluorocarbon substituents substantially elevates the clearing temperatures and facilitates the formation of a columnar phase. The highest Col_h phase stability is displayed by the copper complex **III-4** for which the melting point is below room temperature and the mesophase temperature range is over 240 K. This is in agreement with our previous observation of greater stability for the columnar Col_h phase of copper over nickel complexes and this was attributed to the wider coordination plane for the copper ion [16].

For selected compounds the nature of the liquid crystalline phases observed was confirmed using X-ray diffraction and the measured structural distances are listed in table 4. In the SmC phase the layer spacing is, as usual, much smaller than the molecular length (32 Å for **I-1** compound).

In the case of the hexagonal columnar Col_h phase (**II-2**, **III-3**) the sharp reflections in the low angle region were indexed to the crystallographic indices of a centred planar rectangular lattice, which describes the hexagonal columnar arrangement and gives the measured crystallographic length ratio of the signals (2 0 0)/(0 2 0) = 1.73. The calculated inter-columnar distance from the X-ray data (26 Å) is smaller than the largest molecular dimension measured for the most stretched conformation giving a disk-like molecule (31 Å). This suggests that in the Col_h phase about four or five carbon atoms of the terminal chains can interdigitate. In the wide angle region one diffuse reflection was found for all the compounds studied and, because of its relatively small diffraction angle, this was assigned to the liquid-like order of the terminal chains. For the perfluorinated compounds the average distance between the terminal chains is much higher than that for compounds having purely hydrogenated chains (4.3–4.6 Å [14, 16]). This is due to the much larger cross-sectional area of a perfluorinated chain (27–35 $Å^2$) in comparison with that of alkyl chains (*c*. 20 $Å^2$) [17]. The diffuse signal associated with the distance between the molecular discs was not seen, and to estimate the Col_h phase density the third dimension of the crystallographic cell $c = 3.5$ Å was assumed to be similar to that

Table 4. Structural distances (in Å) obtained using X-ray diffraction (in parentheses) and values calculated from the hexagonal crystallographic cell.

Complex	Phase	Low angle signal			High angle	Cell dimensions
I-1	Sm C	(0 0 1)	(0 0 2)		4.3	
		26.4	13.3			
II-2	Col_h	(1 1 0) = (2 0 0)	(0 2 0) = (3 1 0)	(2 2 0) = (4 0 0)	5.1	$a = 45.6$
		22.8	13.2	11.4		$b = 26.4$
III-3	Col_h	(1 1 0) = (2 0 0)	(0 2 0) = (3 1 0)	(2 2 0) = (4 0 0)	5.5	$a = 46.3$
		23.2	13.4	11.6		$b = 26.8$

of previously synthesized enaminoketone derivatives [14, 16]. Taking into account that in the single crystallographic cell there are two molecules, the calculated density for the columnar phase of **II-2** and **III-3** was 1.38 and 1.29 $g\,cm^{-3}$, respectively. These densities are rather high, and may arise from replacing the hydrogens by fluorine atoms. If the measured distances by X-ray in the wide angle region are also considered to be the distance between two molecular discs along the column, the estimated density for the Col_h phase becomes 0.93 and 0.80 $g\,cm^{-3}$ for **II-2** and **III-3**, respectively. These values seem to be too small and not realistic for compounds containing fluorine atoms. Thus the real densities are probably between these two sets of values.

4. Conclusions

Three series of tetradentate *cis*-enaminoketone complexes, some containing fluorinated terminal chains, have been synthesized. For these compounds both the molecular contour and the type of chain have been modified. Incorporating perfluorinated chains leads to the appearance of more ordered and more stable mesophases due to the incompatibility and microsegregation of the various molecular parts. However, the calamitic phases formed by compounds of series **I** are destroyed by the fluorination of the aliphatic chains and molecular microsegregation is not observed. The compounds studied have triangular mesogenic cores and due to steric reasons the lamellar phases formed by them require an alternating core arrangement in the centre of the layer, figure 1 (*a*). This core packing results in liquid-like paraffinic sub-layers. In the case of the fluorinated compounds the 'paraffinic layer' would consist of mixed hydrocarbon and fluorocarbon chains, figure 1 (*b*). The repulsive forces between perfluoroalkyl chains, as well as poor space filling by fluorinated and non-fluorinated chains, destroy the layer structure, preventing formation of a mesophase.

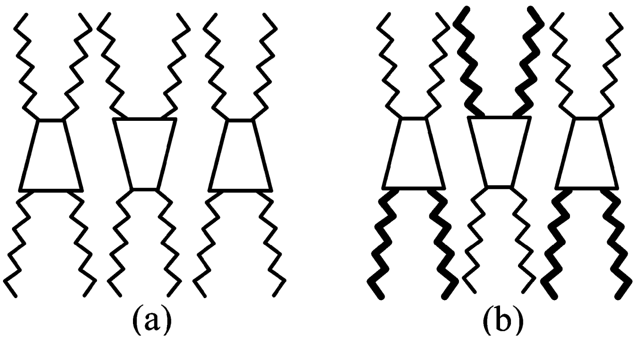

Figure 1. Schematic representation of the smectic layer of series **I** compounds with (*a*) paraffinic and (b) perfluorinated chains; structure (b) is not observed. Thin lines denote alkoxy chains, bold lines denote perfluorinated chains.

For compounds of series **II** and **III** the fluorination of the alkyl chains results in the appearance of a columnar Col_h phase, although separated areas of fluorinated and non-fluorinated chains are not formed. In X-ray studies no additional superstructure was detected. In the columnar phase formed, the terminal perfluorinated and alkyl chains are probably organized in a homogenously mixed system. The shape anisotropy and the van der Waals forces stabilizing the intra-columnar structure are stronger than microsegregation induced by the unlike chains. The columnar structure is promoted by the effective broadening of the mesogenic core which is induced by the substituted fluorocarbon chains. The perfluorinated chains are more rigid than their linear hydrocarbon analogues because of the higher energy barrier between the *trans*- and *gauche*-conformations (9.1 $kJ\,mol^{-1}$) than found for simple alkyl chains (3.4 $kJ\,mol^{-1}$) [18]. This effectively gives more extended and more disk-like molecules with stretched terminal chains which can stabilize the hexagonal columnar phase.

Acknowledgements

The work was supported by KBN Grant No 4T09A00425.

References

[1] B.E. Smart. In *Organofluorine Chemistry Principles and Commercial Applications*, R.E. Banks, B.E. Smart, J.C. Tatlow (Eds), p. 57, Plenum Press, New York (1994).
[2] C. Viney, T.P. Russell, L.E. Depero, R.J. Twieg. *Mol. Cryst. Liq. Cryst.*, **168**, 63 (1989).
[3] C. Vinney, R.J. Twieg, B.R. Gordon, J.F. Rabolt. *Mol. Cryst. Liq. Cryst.*, **198**, 285 (1991).
[4] H.T. Nguyen, G. Sigaud, M.F. Achard, F. Hardouin, R.J. Twieg, K. Betterton. *Liq. Cryst.*, **10**, 389 (1991).
[5] T. Doi, Y. Sakurai, A. Tamatani, S. Takenaka, S. Kusabashi, Y. Nishihata, H. Terauchi. *J. Mater. Chem.*, **1**, 169 (1991).
[6] S.V. Arhart, C. Pugh. *J. Am. Chem. Soc.*, **119**, 3027 (1997).
[7] D. Lose, S. Diele, G. Pelzl, E. Dietzmann, W. Weissflog. *Liq. Cryst.*, **24**, 707 (1998); E. Nishikawa, J. Yamamoto, H. Yokoyama. *J. Mater. Chem.*, **13**, 1887 (1991).
[8] M.A. Guillevic, D.W. Bruce. *Liq. Cryst.*, **27**, 153 (2000).
[9] J.P. Bedel, J.C. Rouillon, J.P. Marcerou, M. Laguerre, T.H. Nguen, M.F. Achard. *J. Mater. Chem.*, **12**, 2214 (2002).
[10] C. Tschierske. *J. Mater. Chem.*, **11**, 2647 (2001).
[11] J. Mu, H. Okamoto, T. Yanai, S. Takenaka, X. Feng. *Colloids and Surfaces A*, **181**, 303 (2001).
[12] A. Pegenau, X.H. Cheng, C. Tschierske, P. Göring, S. Diele. *New J. Chem.*, **23**, 465 (1999).
[13] X.H. Cheng, S. Diele, C. Tschierske. *Angew. Chem. Int. Ed.*, **39**, 592 (2000).

[14] U. Pietrasik, J. Szydłowska, A. Krówczyński, D. Pociecha, E. Górecka, D. Guillon. *J. Am. Chem. Soc.*, **124**, 8884 (2002).

[15] J. Szydłowska, A. Krówczyński, E. Górecka, D. Pociecha. *Inorg. Chem.*, **39**, 4879 (2000).

[16] A. Krówczyński, J. Szydłowska, D. Pociecha, J. Przedmojski, E. Górecka. *Liq. Cryst.*, **1**, 117 (1998).

[17] C. Tschierske. *J. Mater. Chem.*, **8**, 1485 (1998).

[18] J-W. Lee, Y. Park, J-I. Jin, M.F. Achard, F. Hardouin. *J. Mater. Chem.*, **13**, 1367 (2003).